

# Coarse-Fine Residual Gravity Cancellation System with Magnetic Levitation

S.E. Salcudean  
Department of Electrical Engineering  
University of British Columbia  
Vancouver, BC, V6T 1Z4, Canada

H. Davis, C.T. Chen, D.E. Goertz  
Department of Physics  
University of British Columbia  
Vancouver, BC, V6T 1Z1, Canada

B.V. Tryggvason  
Canadian Astronaut Program, Canadian Space Agency  
Rockliffe Base, Ottawa, Ont., K1A 1A1, Canada

## Abstract

*This paper describes a six degrees-of-freedom active experiment isolation system designed to cancel out residual accelerations during "zero-g" parabolic flights (e.g., NASA KC-135 flights). The isolation system consists of a fine-motion magnetic levitator whose stator is transported by a conventional coarse-motion stage or by a robot. The levitator uses wide-gap voice-coil actuators and has the dual purpose of isolating the experiment platform from aircraft vibrations and actively cancelling residual accelerations through feedback control. The robot tracks the levitated platform in order to keep the levitator's coils centered within their matching magnetic gaps. Aspects of system design, an analysis of the proposed control strategy and simulation results are presented. Feasibility experiments using a PUMA 500 and a magnetically levitated robot wrist are also discussed.*

## 1 Introduction

A number of scientific experiments require zero-gravity conditions. As an alternative to outer-space experiments and drop-towers, aircraft flights along parabolic trajectories have been executed in order to achieve low-cost, near free-fall conditions of moderate duration. During such parabolic flights, equipment that is solidly attached to the aircraft is still subject to small, unwanted, forces, due to aircraft trajectory errors (low frequency components) and to mechanical vibrations (high frequency components).

In order to deal with aircraft trajectory errors, large motion isolation mounts (LMIMs) have been proposed and tested [1, 2, 3]. These consist of low-friction large-motion sliders ( $z$ -motion only,  $x - y$  gantry with additional  $z$ -motion) that allow an experiment to freely move within an engaged volume within the aircraft. Active gravity cancellation has also been proposed and can be achieved by using linear motors to actuate one or several of the slider's degrees of freedom (DOF) [3].

This paper proposes a coarse-fine residual gravity cancellation system that completely isolates the platform carrying the zero-g experiment from the aircraft frame. The system uses magnetic levitation for small, high frequency motion isolation, combined with

a coarse positioning robot for large amplitude, low frequency motion isolation. Coarse-fine motion systems have been proposed, analyzed and used before for increasing speed and dexterity in manufacturing tasks [4, 5, 6, 7]. Although the system proposed here is similar to the one presented in [7, 8], the work presented in this paper differs from what was previously reported in several ways. First, the specific problem of active zero-g control through acceleration feedback is considered and analyzed. Second, 6 DOF coarse-fine motion coordination schemes are proposed, analysed and simulated with realistic assumptions on the performance of the coarse and fine motion stages. Finally, 6 DOF tracking of a levitated platform by a coarse-motion stage is experimentally demonstrated for the first time. A PUMA 500 equipped with a magnetically levitated wrist were used for this purpose.

This paper is organized as follows: In Section 2, the new coarse-fine vibration isolation system for micro-gravity experiments is proposed and some overall design ideas are presented. In Section 3, the coarse-fine motion system is modelled. Control and coordination algorithms are also proposed and analysed. These involve acceleration feedback and the use of coarse and fine sensors for tracking of the free-falling experiment platform. In Section 4, motion simulation results, using measured acceleration data from NASA KC-135 parabolic flights, are presented under realistic design assumptions. In Section 5, the experimental setup used to demonstrate the feasibility of the proposed system is described and the experiments performed to date are summarized. Both simulations and experiments demonstrate that a coarse-fine motion isolation system with magnetic levitation is feasible.

## 2 Coarse-Fine Isolation Mount Design

There are several possible approaches to isolating the experiment platform from the aircraft carrying it. The simplest solution is just to allow the platform to float inside the aircraft, while tracking it with a coarse motion stage and latching it at the end of the free-fall parabola or whenever necessary. However, there are several good reasons to consider an active vibration isolation system. These include the ability to can-

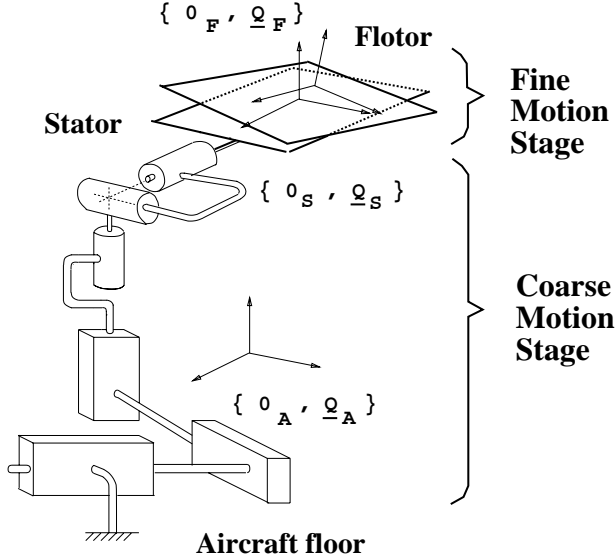


Figure 1: Overview of the vibration isolation system.

cel disturbances on the experiment platform, such as pulling forces by data collection and power wires, inadvertent touching of the experiment by an operator, or motion caused by reaction forces due to the experiment itself. In addition, an active isolation system would allow a controlled zero acceleration release at a desired instant and at a specific location in the airplane, and therefore allows one to maximize the duration of free-fall of a package before it hits the aircraft walls [1, 2, 3]. Finally, an active large motion isolation system would allow the exertion of small centering forces on the experiment platform, in effect trading acceleration levels for experiment duration. This ability would gain in importance if the aircraft acceleration levels on parabolic flights could be decreased through better sensing and control.

Active vibration isolation solutions that involve direct mechanical linkages and also allow some controlled exertion of forces would be difficult to design and implement because the actuator exerting the force would also transmit unwanted vibrations. Thus some active levitation method is desirable because it would allow low cutoff frequency low-pass filtering of the actuation forces. Such active levitation methods could involve magnetic-bearing type of actuators with iron in the magnetic gap, or "voice-coil" actuators (or Lorentz actuators) with conductors in the magnetic gap. The latter has several advantages, some of which are the need for just a single actuator for bi-directional motion along each DOF, the linearity of applied force with command current and the simplicity of design.

The overview of the proposed system, whose concept follows closely [7], is given in Figure 1. A coarse motion stage, attached to the aircraft body, can impart fast, controlled, 3-DOF (or more) motion to the *stator* of a levitator. For simplicity, the coarse-motion stage shown in Figure 1 is a cartesian robot of the gantry type equipped with a spherical wrist, but there is considerable freedom in choosing its structure. In

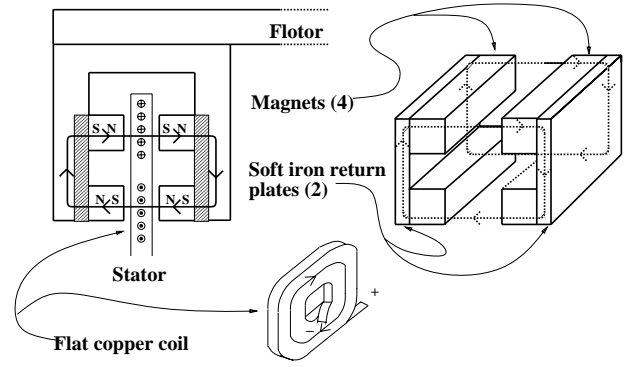


Figure 2: Lorentz actuator schematic.

keeping with the terminology proposed in [7], the levitated experiment platform is referred to as the *flotor*, and is actuated by at least six wide-gap Lorentz actuators, shown in Figure 2.

Each actuator has a magnetic assembly, attached to the flotor and a matching coil, attached to the stator. The limited size of the magnetic gaps allows only limited motion of the flotor with respect to the stator ( $\pm 20 - 30$ mm in translation). Although the flotor is not physically attached to the stator (except, perhaps, for wires carrying signals and power) controlled forces can be imparted to the platform by controlling the coil currents. With a suitably chosen geometry, 6 DOF motion in any direction can be achieved without excessive coil currents [7].

Even with the best available technology, it would be very difficult, if not impossible, for the levitator's actuators to produce enough force to support the entire weight of the flotor under normal gravity conditions. Thus, a latch mechanism is necessary to anchor the flotor under normal (or higher than normal) gravitational accelerations. The position of the flotor with respect to the stator can be obtained by an optical sensor similar to the ones presented in [9, 8, 7].

### 3 Modelling and Control

The following coordinate systems are defined and shown in Figure 3:  $\{o_A, \mathbf{Q}_A\}$ , attached to the aircraft frame at the nominal center of the robot workspace,  $\{o_S, \mathbf{Q}_S\}$ , attached to the levitator's stator,  $\{o_F, \mathbf{Q}_F\}$ , attached to the flotor's center of mass and aligned about its principal axes of inertia, and an inertial system  $\{o_I, \mathbf{I}\}$ , whose origin coincides with  $o_A$  at the start of the free-fall parabola. When the flotor is in its nominal position, the flotor and stator coordinate systems coincide, and the identity matrix  $\mathbf{I}$  is chosen as illustrated in Figure 3, with the  $z$ -axis being aligned with the gravitational force, and the initial aircraft velocity lying in the  $xz$ -plane. ( $\mathbf{g} = [00 - 9.81]^T$ ). All vectors and matrices expressed in the inertial system will be shown in bold letters.

It is assumed that the flotor (and the experimental platform it carries) can be accurately modelled by a rigid body having mass  $m$  and inertia matrix with respect to its center of mass  $\mathbf{J}$ . In flotor coordinates, the inertia matrix becomes  $J = \mathbf{Q}_F^T \mathbf{J} \mathbf{Q}_F$ . Let  $\mathbf{a}$  and

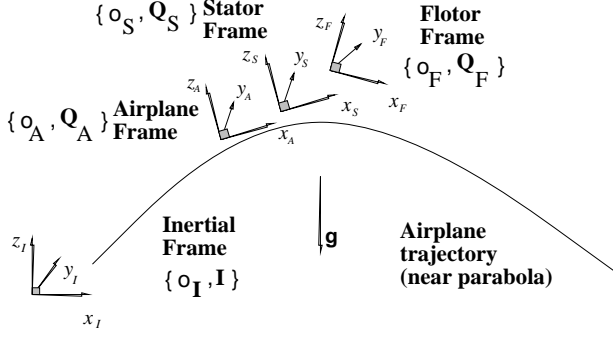


Figure 3: Coordinate systems used in the model.

$a = \mathbf{Q}_F^T \mathbf{a}$ ,  $\omega$  and  $\omega = \mathbf{Q}_F^T \boldsymbol{\omega}$  denote the flotor's acceleration and angular velocity in inertial and, respectively, flotor coordinates, let  $\mathbf{f}$  denote the force acting on the flotor, and let  $\boldsymbol{\tau}$  denote the torque acting at the flotor's center of mass.

In flotor coordinates, the flotor's dynamics are described by Newton's law and Euler's equation:

$$m\mathbf{a} = m\mathbf{g} + \mathbf{f} + \mathbf{f}_d; \quad J\dot{\boldsymbol{\omega}} + \boldsymbol{\omega} \times J\boldsymbol{\omega} = \boldsymbol{\tau} + \boldsymbol{\tau}_d, \quad (1)$$

where  $\boldsymbol{\omega} = \mathbf{Q}_F \boldsymbol{\omega}$ ,  $\mathbf{f} = \mathbf{Q}_F \mathbf{f}$ ,  $\mathbf{g} = \mathbf{Q}_F \mathbf{g}$ ,  $\boldsymbol{\tau} = \mathbf{Q}_F \boldsymbol{\tau}$ , and  $\mathbf{f}_d = \mathbf{Q}_F \mathbf{f}_d$  and  $\boldsymbol{\tau}_d = \mathbf{Q}_F \boldsymbol{\tau}_d$  are disturbance forces and torques (from eddy-current coupling between flotor and stator, flow of air, dragging power wires, etc), and the flotor's kinematics is described by

$$\frac{d}{dt} \mathbf{Q}_F = \boldsymbol{\omega} \times \mathbf{Q}_F; \quad \boldsymbol{\omega} \times = \begin{bmatrix} 0 & -\omega_3 & \omega_2 \\ \omega_3 & 0 & -\omega_1 \\ -\omega_2 & \omega_1 & 0 \end{bmatrix}. \quad (2)$$

The tracking robot should have at least three, but preferably six, DOFs. It is assumed that the robot has a closed-loop controller that servo the stator's position and orientation with respect to the aircraft frame, *i.e.*, that the coordinates  ${}^A r_{AS}$  of  $o_S - o_A$  in  $\mathbf{Q}_A$  frame ( $o_S - o_A = \mathbf{Q}_A {}^A r_{AS}$ ) and  $\mathbf{Q}_S^{-1} \mathbf{Q}_A = \mathbf{Q}_S^T \mathbf{Q}_A$  are available and controllable. A reasonable assumption on the behaviour of the the stator position under feedback control is that of a second order system with limits on velocity and acceleration:

$${}^A \ddot{r}_{AS} + 2\zeta\omega_0 {}^A \dot{r}_{AS} + \omega_0^2 {}^A r_{AS} = \omega_0^2 {}^A r_{AS_d} \quad (3)$$

$$\| {}^A \ddot{r}_{AS} \| < a_{max}; \quad \| {}^A \dot{r}_{AS} \| < v_{max} \quad (4)$$

where  $\omega_0$  determines the cutoff frequency at which the stator can no longer track the command input  ${}^A r_{AS_d}$  and the damping coefficient  $\zeta$  determines the overshoot of the response. Similar assumptions can be made on the stator orientation servo by using some appropriate orientation parametrization. For the sake of simplicity, the parameters in the above equations were taken to be the same for each motion axis.

It will be assumed that the disturbance forces exerted on the stator in reaction to forces applied by the

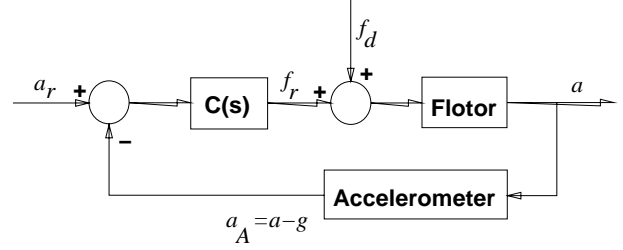


Figure 4: Flotor acceleration feedback.

levitator, as well as the effects of the aircraft motion, have negligible effects on the coarse-stage motion. If this is not the case, a detailed stability analysis of the coupled motion of the coarse and fine systems should be done along the lines of the work presented in [6]. During the free-fall part of the flight, the acceleration levels do not exceed 50 mg [10], so even with a heavy experiment platform (300 lb or so), the forces required to completely stop the platform motion are quite small.

In order to prevent the flotor from exceeding its motion range, during the free-fall part of the aircraft flight, the commanded stator position should always coincide with that of the flotor, *i.e.*,  ${}^A r_{AS_d} = {}^A r_{AF}$ , where  $o_F - o_A = \mathbf{Q}_A {}^A r_{AF}$ . The coordinates  ${}^A r_{AF}$  can be obtained from the combined measurements of the stator position with respect to the aircraft (through the conventional sensors of the coarse-motion stage or robot) and that of the flotor position with respect to the stator (through the levitator's optical sensor).

### 3.1 Flotor Acceleration Feedback

It is assumed that the acceleration of  $o_F$  is measured by accelerometers attached to the flotor. Once it is released, the force on the flotor is some compensated function of the acceleration error, as shown in Figure 4. In terms of Laplace transforms,

$$\hat{f}(s) = \hat{c}(s)(\hat{a}_r(s) - \hat{a}(s)), \quad (5)$$

where  $\hat{c}(s)$ ,  $\hat{a}(s)$  and  $\hat{a}_r(s)$  are the Laplace transforms of the feedback compensator, the flotor acceleration and the required acceleration, respectively. Due to the simplicity of the flotor dynamics, *any* proper, stable, real-rational transfer function can be obtained from the desired acceleration  $a_r$  to the actual acceleration  $a$  of the flotor (of course, there will be limits on achievable performance due to plant uncertainty, actuator saturation, etc.). Choosing a first order stable transfer function leads to a compensator  $\hat{c}(s)$  that is simply an integrator, *i.e.* it implements *velocity* feedback:

$$\hat{f}(s) = k \frac{1}{s} (\hat{a}_r(s) - \hat{a}(s)), \quad (6)$$

which leads to

$$\hat{a}_A(s) = \frac{\frac{k}{m}}{s + \frac{k}{m}} [\hat{a}_r(s) - g] + \frac{\frac{1}{m}s}{s + \frac{k}{m}} \hat{f}_d(s). \quad (7)$$

where the signal  $a_A = a - g$  (zero in free fall) is provided by a proof-mass accelerometer.

Clearly, for reasonably high gain  $k$ , the acceleration of the flotor and platform *does indeed track the desired acceleration*  $a_r$  and *rejects the disturbance force*  $f_d$ . Usually,  $a_r = g$ , leading to  $\hat{a}_A(s) \rightarrow 0$ , although, as it will be seen later, this may not always be the best approach.

The angular acceleration of the flotor can be controlled in a similar way, *i.e.*, by using angular velocity feedback. Indeed, let  $\tau = -k_\omega J\omega$ , with  $k_\omega$  positive, and consider the Lyapunov function  $V = \frac{1}{2}\omega^T J\omega$ . Along the trajectories of Euler's equation in (1) (with  $\tau_d = 0$ ),

$$\begin{aligned} \dot{V} &= \frac{1}{2}[\omega^T(\tau - \omega \times J\omega) + (\tau - \omega \times J\omega)^T\omega] \\ &= \omega^T\tau = -k_\omega\omega^T J\omega < 0 \end{aligned} \quad (8)$$

and therefore the signal  $\delta = -\omega \times J\omega$  is bounded and decreases to zero. With  $a_\omega = \dot{\omega}$ , the Laplace transform of Euler's equation leads to

$$\hat{a}_\omega(s) = \frac{s}{s + k_\omega} J^{-1}\hat{\delta}(s), \quad (9)$$

from which it follows that the angular acceleration of the flotor will be kept small at low frequencies.

Before moving on, a comment on the nature of the disturbances acting on the flotor (or experimental platform) and the means of rejecting them is in order. On one hand, disturbance forces can be both unknown and very difficult to measure, *e.g.* forces due to an experiment operator touching the flotor. The only hope of attenuating these disturbances is through accelerometer feedback. On the other hand, some unpredictable disturbances can be easily measured, *e.g.* the forces and torques applied to the flotor by an umbilical carrying signals and power. These disturbances can be rejected to a large extent through *feed-forward through the flotor's actuating coils*, while accelerometer feedback is still in effect.

Umbilical disturbances can be measured by means of standard strain-gauge force-torque sensors or through other, more sophisticated, techniques. Even magnetic levitation can be used, with the same proof-mass/force-balance principle used in some accelerometers. For example, the umbilical can be attached to the flotor through an intermediate levitated proof-mass (*i.e.*, another flotor), whose position and orientation is servoed to that of the experimental platform. By monitoring the forces needed to keep the proof-mass in place (*e.g.*, by monitoring the coil currents of Lorentz actuators, if the proof-mass uses Lorentz levitation), one obtains the forces and torques exerted by the umbilical.

### 3.2 Acceleration Feedback with Centering Motion

Although, ideally, the desired flotor acceleration  $a_r$  is zero, in practice, even the tracking robot will "run out of space" because of errors in the aircraft trajectory. Instead of letting the platform reach its motion limit (with associated high acceleration due to

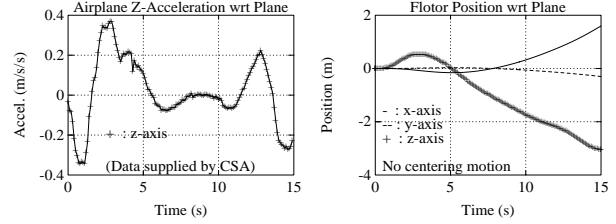


Figure 5: The position of the platform with respect to the airplane with a given disturbance in the z-axis of the airplane.

hard mechanical contact), it may be instead desirable to provide low-level "drift" accelerations that tend to bring the flotor to the nominal center of the coarse motion platform. It will be assumed that this nominal center coincides with the aircraft reference frame origin  $o_A$ . There are a couple of ways in which a centering drift motion can be obtained. First, one can modify the control action (6) by adding a proportional derivative term in the flotor offset  $r_{FA} = \mathbf{Q}_F^T(o_A - o_F)$  with respect to the aircraft frame:

$$\hat{f}(s) = k \frac{1}{s} [\hat{a}_r(s) - \hat{a}(s)] + k_p \hat{r}_{FA}(s) + k_v s \hat{r}_{FA}(s), \quad (10)$$

where  $k_p$  and  $k_v$  are positive and small. To see what is the effect of this centering force, one can let  $k = 0$  in the above and use Newton's equation to obtain that

$$m \frac{d^2}{dt^2}(o_F - o_I) = m\mathbf{g} + \mathbf{Q}_F(k_p r_{FA} + k_v \dot{r}_{FA}) + \mathbf{f}_d. \quad (11)$$

Therefore, in inertial coordinates, the equation of motion of the flotor origin with respect to the aircraft frame becomes

$$\begin{aligned} \frac{d^2}{dt^2}(o_F - o_A) + \frac{k_v}{m} \frac{d}{dt}(o_F - o_A) + \frac{k_p}{m}(o_F - o_A) \\ = \frac{k_v}{m} \omega \times (o_F - o_A) + \frac{1}{m} \mathbf{f}_d, \end{aligned} \quad (12)$$

where use was made of the facts that

$$\frac{d}{dt}(o_F - o_A) = \omega \times (o_F - o_A) + \mathbf{Q}_F \dot{r}_{FA}$$

and, since aircraft trajectory errors are included in  $\mathbf{f}_d$ ,

$$\frac{d^2}{dt^2}(o_A - o_I) = \mathbf{g}. \quad (13)$$

Even without angular acceleration servoing, the flotor's angular velocity  $\omega$  is small because the aircraft rotates slowly during the parabolic flight. In addition, due to the orthogonality of  $\omega \times (o_A - o_F)$  to the centering force  $\frac{k_p}{m}(o_F - o_A)$  acting on the flotor, it should be possible to use a Lyapunov argument to show that, in the absence of disturbance forces  $\mathbf{f}_d$  and assuming that  $\omega$  is bounded,  $o_F - o_A$  converges to zero. Therefore, by using *only local* information (*i.e.*, no inertial

reference) the flotor can be made to track the aircraft center. In order to insure low accelerations, the constants  $k_p$  and  $k_v$  should be made as small as possible.

As a second way to achieve a centering force on the flotor, note that the desired acceleration  $a_r$  of (6) can be set according to a PD law similar to (10), *i.e.*,

$$\hat{a}_r(s) = k_p \hat{r}_{FA}(s) + k_v s \hat{r}_{FA}(s). \quad (14)$$

If the acceleration controller works well,  $a$  should track  $a_r - g$  closely (see equation (7)), so, in effect, (10) will be quite well approximated. Of course, for such an approach to work, the acceleration gain of (6) should lead to a substantially faster time constant than the time constants associated with (14).

It is also possible to make the gains  $k_p$  and  $k_v$  depend on how close the platform is to the aircraft walls - the larger  $o_F - o_A$ , the larger  $k_p$  and  $k_v$ . In particular, a moderately large workspace without drift can be implemented by setting these gains to zero within a certain radius  $\|o_F - o_A\| < r$ .

A corrective term for drift in the orientation of the platform can also be devised. In particular, if the coarse-motion stage is only a 3-DOF system, as the airplane goes through a parabola, the levitator's stator will change orientation with it. Therefore, in spite of being free to move in translation, *the flotor orientation must track that of the stator*. Tracking could be achieved by using a control scheme based on the vector part of the Euler quaternion, as done in [7]. The relative rotation  $Q_{AF} = \mathbf{Q}_A^T \mathbf{Q}_F$  of the flotor with respect to the aircraft is represented by the Euler quaternion  $[\beta_0 \beta^T]^T = [\cos(\phi/2) \sin(\phi/2)s^T]^T$ , where  $s$  and  $\phi$  are the rotation axis ( $\|s\| = 1$ ) and, respectively, the rotation angle of  $Q_{AF}$ . It can be shown [7] that, after (approximate or exact) linearization the flotor's rotational dynamics are given by

$$\ddot{\beta} = \frac{1}{2} J^{-1} \tau. \quad (15)$$

Therefore, a PD term similar to (10) can be added to the flotor torque in such a way as to bring the orientation of the flotor towards some central orientation aligned with the aircraft:

$$\tau = -\tilde{k}_p \beta - \tilde{k}_v \dot{\beta}, \quad (16)$$

where the orientation vector  $\beta$  corresponding to to  $\beta_0 \geq 0$  can be obtained from  $Q_{AF}$  [7].

It is clear that, when the platform acceleration is not measured, there can be no acceleration error correction for the platform. The robot can still be used to track the platform and the moving coil actuators can still be used to center the flotor.

## 4 Simulation Setup and Results

The motion of the system described in Section 2, with the control laws described in Section 3, was simulated using the software packages PRO-MATLAB<sup>TM</sup> and SIMULAB<sup>TM</sup>, by The MathWorks. Acceleration data obtained on NASA KC-135 parabolic flights [10] were used to obtain the aircraft position. Although

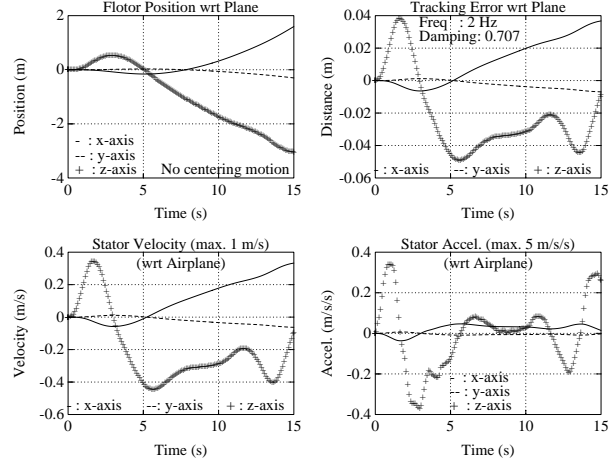


Figure 6: Flotor-stator tracking errors.

there was no measured data available on the orientation of the KC-135 during flight, the initial aircraft orientation at the start of the parabola and the final orientation at the end of free-fall are fairly well known. These show that the aircraft undergoes a change in pitch angle of about  $-60^\circ$  and is rolling to the right roughly  $20^\circ$  during the free-fall parabola. In all the simulations performed, it was assumed that this rotation occurs at a constant angular rate, about the fixed Euler eigenaxis of rotation between the initial and final orientations.

Typical results are displayed in Figures 5, 6, 7 and 8. Unless otherwise specified, airplane coordinates are used. Figure 5 shows the acceleration data and the flotor position. Figure 6 shows the tracking errors in  $x$ ,  $y$ ,  $z$ . As expected, the coarse-motion stage tracking error along the  $z$ -axis is substantially larger than for the  $x$  and  $y$  axis. With fairly stringent performance limitations on the coarse motion stage (2 Hz bandwidth, 5 m/s/s max. acceleration, 1 m/s max. velocity), typical tracking errors are about  $\pm 10$  mm in the  $y$ -axis,  $\pm 30$  mm in the  $x$ -axis and  $\pm 40$  mm in the  $z$  axis. These errors are reduced drastically as the bandwidth of the tracking platform is increased. It is fairly simple to design a wide-gap levitator that matches these workspace requirements. For example, the stator could be shaped as a rectangular shell with flat coils (as shown in Figure 2) embedded in its walls. The matching flotor would have a large face available for an experiment platform, and would have a substantial travel in the  $z$  axis, while maintaining relatively small magnetic gaps for the actuators.

Figure 7 shows the rotation tracking performance (the three components of the vector part  $\beta$  of the Euler quaternion, defined in Section 3, are displayed) and the torques applied to the flotor. It can be seen that the orientation errors are small and that the torques required to rotate the flotor are small (the flotor is modelled as a 300 lb cube, which is the expected experimental platform weight).

Figure 8 shows the trade-off between acceleration quality and free-fall duration. Simulation results with

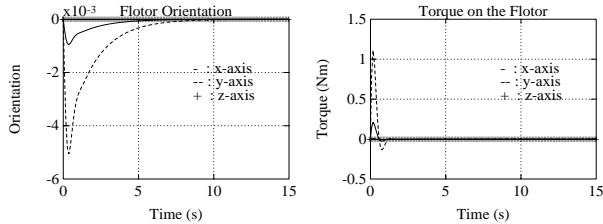


Figure 7: Orientation errors flotor torque.

two sets of centering gains in equation (14) are displayed. It can be seen that as these gains are increased, the flotor moves less with respect to the aircraft. At the same time, the acceleration levels on the flotor increase, as expected. If the required acceleration level for a given experiment is known, one can modify the centering acceleration of equation (14) in order to optimize experiment duration. Another possible use for centering forces is the avoidance of "crashes" into the aircraft walls.

## 5 Experimental Setup and Results

To demonstrate the feasibility of the coarse-fine motion isolation system the authors used a Unimation PUMA 500 robot equipped with a magnetically levitated fine-motion robot wrist, developed and built in the Electrical Engineering Department at UBC. The UBC maglev wrist [11] uses the same design principles applied to the "Magic" wrist described in [7, 8] and outlined in Section 2 of this paper. The real-time system employed for the coordinated control of the PUMA robot and the levitator's flotor is illustrated in Figure 9.

An IBM PC-AT compatible computer hosts a Spectrum Inc. digital signal processing (DSP) board using a Texas Instruments Inc. TMS320 DSP chip, as well as analog input and output boards linked through a fast, private bus. The PC is connected through a 19.2 Kbaud serial link to the PUMA robot controller.

The floating point DSP board performs several functions. It controls the levitator's flotor, computes the stator's position and orientation (from position and Euler angles information obtained from the robot through the serial link), and calculates the updated robot set points ( $\delta x$ ,  $\delta y$ ,  $\delta z$ , roll, pitch, yaw) as a function of flotor position. The kinematic calculations required to determine the flotor position with respect to the stator are exactly as described in [7]. The flotor controls are updated every 1.5 milliseconds, with the DSP board running at about 1 Mflop.

The PC is used for DSP software development and for the serial port communications between the wrist controller and the robot controller.

A program written in VAL II handles the serial communications on the PUMA controller side, while the robot is in INTERNAL ALTER mode, effectively making it a slave to the wrist's flotor motion. The coordination data between the robot and the wrist could only be transmitted every 56 milliseconds. This could be improved substantially if the the PUMA controller could be modified. In particular, a Jacobian-based ve-

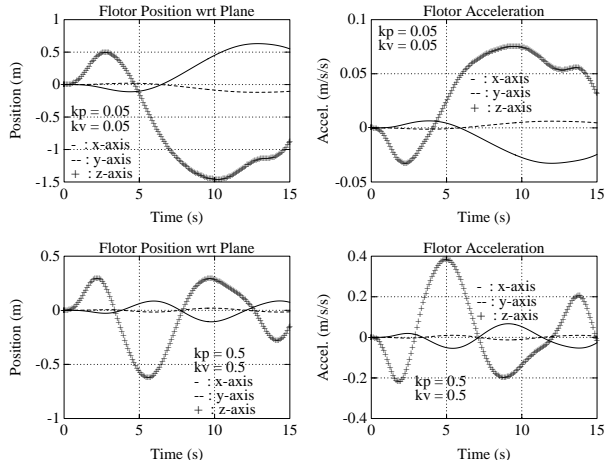


Figure 8: Effects of centering control on position and acceleration.

locity tracking algorithm that does not require the on-line solution of the inverse kinematics problem could be implemented.

Coordinated motion of the flotor and the robot was demonstrated by the authors, with the robot following the wrist's flotor position and orientation. Translational tracking with locked orientation was also demonstrated.

Accelerometers were mounted on the flotor, but problems with drift and noise have so far prevented successful implementation of acceleration feedback.

## 6 Conclusion

The authors proposed a coarse-fine large-motion isolation system for residual gravity cancellation on parabolic flights. The system uses wide gap magnetic levitation for vibration isolation and acceleration servoing of an experimental platform, as well as a coarse-motion tracking robot to provide a "support point" against which the flotor actuators can act. The proposed isolation mount was modelled and control algorithms for acceleration servoing and centering motion were presented. The model and the control algorithms were simulated and an experimental coarse-fine system using a PUMA robot and maglev wrist was put together in order to demonstrate the system's feasibility.

The proposed gravity cancellation system has several advantages, among which are (i) the ability of removing the dynamic coupling between the aircraft and experimental platform, (ii) the ability of using maglev forces to obtain good initial release of the experiment platform, (iii) the ability of rejecting disturbances on the experimental payload, (iv) the ability of trading off experiment duration versus quality of the free-fall.

The simulation results and experimental results presented seem to indicate that such a coarse-fine approach to vibration isolation is feasible. In particular, the ability of a coarse-motion stage to track a levitated platform was demonstrated through both simulations and experiments. The only requirement left

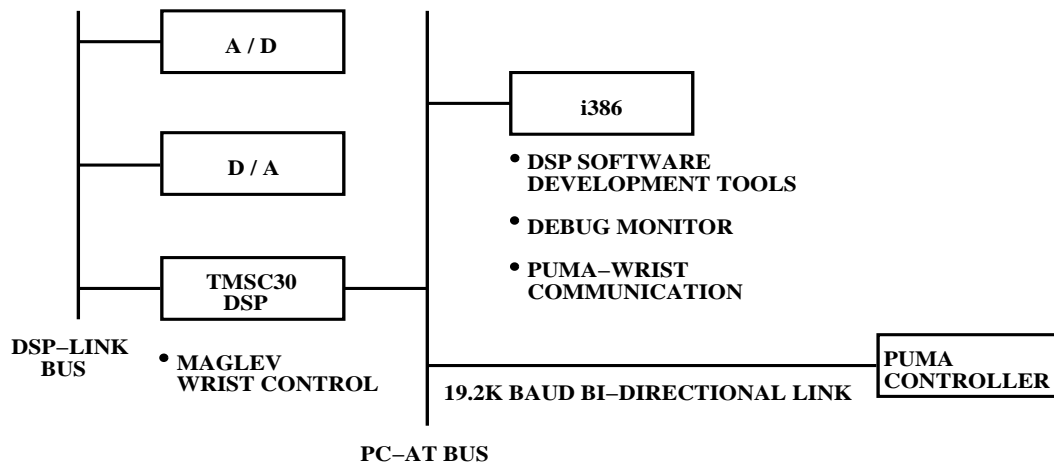


Figure 9: PUMA-Wrist real-time controller.

to demonstrate in order to show that the coarse-fine motion isolation system will work as proposed is the successful application of acceleration feedback. That work is now in progress. In order to quantify the degree of mechanical isolation that can be provided by a system such as the one proposed in this paper, near future plans (June 1992) include flight-testing (on a NASA KC-135 flight) of a one-dimensional coarse-fine motion stage with an accelerometer-equipped maglev wrist.

## 7 Acknowledgements

The authors wish to thank David Fletcher for machining the maglev wrist used in their experiments, Dr. Dale Cherchas for providing space and experimentation time in his lab, and Nelson Ho for general help and for writing the symbolic debug monitor for the DSP. The support of NSERC and the Canadian Space Agency is gratefully acknowledged.

## References

- [1] A. Adler and J. Bernaldez. Motion isolation mount for microgravity. Technical report, Dept. of Physics, University of British Columbia, December 1989. Engineering Physics Project No. 8918.
- [2] H. Davis. Report on the proposed modifications to the 1-d large motion isolation mount for flight tests on the nasa kc-135 aircraft. Technical report, Engineering Physics, University of British Columbia, October 1990. (prepared for NRC under contract 31016-0-6022/01-SW).
- [3] H. Davis. Report on the first flights of the large motion isolation mount on the nasa kc-135 aircraft, june 5-9, 1990. Technical report, Engineering Physics, University of British Columbia, September 15 1990. (prepared for NRC under contract 31016-0-6022/01-SW).
- [4] R. H. Taylor, R. L. Hollis, and M. A. Lavin. Precise manipulation with endpoint sensing. *IBM J. Res. Develop.*, 2(4):363-376, July 1985.
- [5] Andre Sharon and David Hardt. Enhancement of robot accuracy using endpoint feedback and a macro-micro manipulator system. In *American Control Conference proceedings*, pages 1836-1842, San Diego, California, June 6-8 1984.
- [6] S.E. Salcudean and C. An. On the Control of Redundant Coarse-Fine Manipulators. In *Proceedings of the IEEE International Conference on Robotics and Automation*, pages 1843-1840, Scottsdale, Arizona, May 14-18, 1989.
- [7] R.L. Hollis, S.E. Salcudean, and P.A. Allan. A Six Degree-of-Freedom Magnetically Levitated Variable Compliance Fine Motion Wrist: Design, Modelling and Control. *IEEE Transactions on Robotics and Automation*, 7(3):320-332, June 1991.
- [8] R.L. Hollis. Magnetically levitated fine motion robot wrist with programmable compliance, October 1989. U.S. Patent number 4,874,998.
- [9] A.E. Brennemann, R.L. Hollis, and R.H. Taylor. General position and orientation sensor for fine motions and forces. *IBM Technical Disclosure Bulletin*, 26(9):4457-4462, February 1984.
- [10] B. V. Tryggvason. Acceleration Levels on the KC-135. Technical report, Canadian Space Agency, October 1990. Report CSA-CAP.008.
- [11] S.E. Salcudean, N.M. Wong, and R.L. Hollis. A Force-Reflecting Teleoperation System with Magnetically Levitated Master and Wrist. In *Proceedings of the IEEE International Conference on Robotics and Automation*, pages 1420-1426, Nice, France, May 10-15, 1992.